

Examples of calculation in the layered medium.

Sound pulse in the Pekeris' waveguide.

Fig. 1.1 shows the signals from a pulse source received at 0 (in the source), 5, 15 and 20 Km (left right top bottom) in the frequency band from 50 to 60 Hz. Source resides at 68 m depth. The whole waveguide depth is 100 m. The sound speed in water is 1500 m/s, the sound speed in bottom is 1800 m/s and the density in bottom is 1700 kg/m^3 . The solid line stands for the envelope of the exact solution, calculated by the normal mode method. The shading represents the PDPE solution. The time structure of the signal at larger distances clearly exhibits the arrivals of separate modes and the stretch of the pulse widths of each mode due to the frequency dispersion of the mode group velocity. The agreement of the results may be seen as rather good.

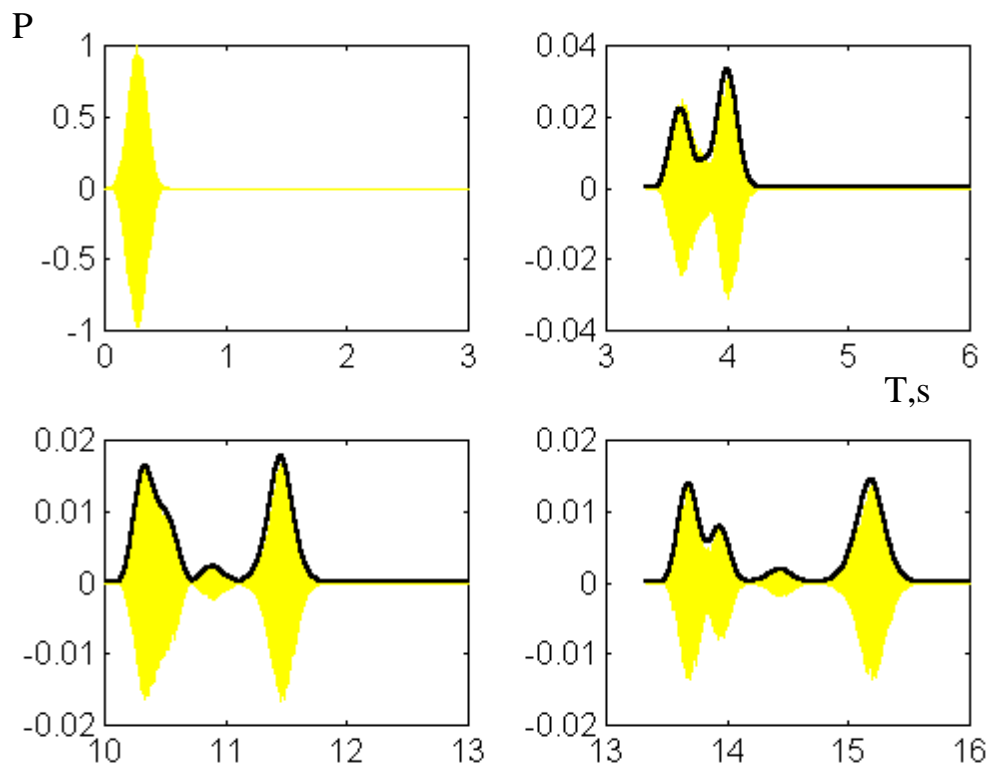


Fig.1. The pulse signals in Pekeris' waveguide.

Field of an explosive sound source in the deep ocean.

Fig. 2.1 shows the sound speed profile in water and bottom typical for the boundary of Gulf stream current in the Atlantic Ocean with two minima. The upper sediment bottom layer is of 0.4 Km depth. The sound speed at its upper boundary is taken less than in water and is linearly increasing with depth according to available geological data ($C(z) = 1.52 + 0.0004 \text{ km/c}$ for z from 4.8 Km to 5.2 Km). The density of sediments increases with depth also linearly.

Fig. 2.2 shows the signal of underwater shot of the charge of 2.8 KG at depth 0.29 Km in the frequency band from 10 to 200 Hz. The distance from the source is 30 Km and receiver depth is 1.2 Km. This signal is calculated by the PDPE technique in a layered model of ocean with the sound speed profile from Fig. 2.1. The signs " + " and " * " designate times of separate arrivals of an explosive signal, calculated by the ray method. Arrivals with greater amplitude are water refracted; those with smaller amplitude are bottom reflected. Fig. 2.3 shows a part of the signal due to the first bottom reflection at the expanded time scale.

Fig. 2.4 shows a fragment of an experimentally registered signal in the same region of Atlantic Ocean due to the first bottom reflection. One can see a rather good agreement of calculated arrival times and of experimental and calculated delays in bottom reflected arrivals.

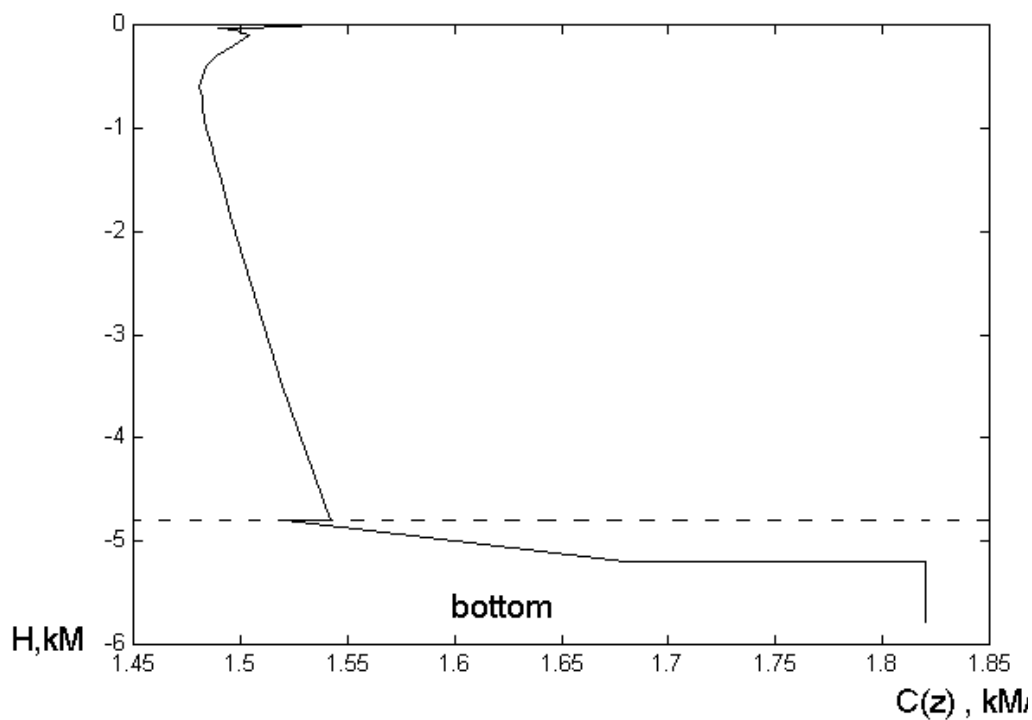


Fig. 2.1 Sound speed profile in water and bottom.

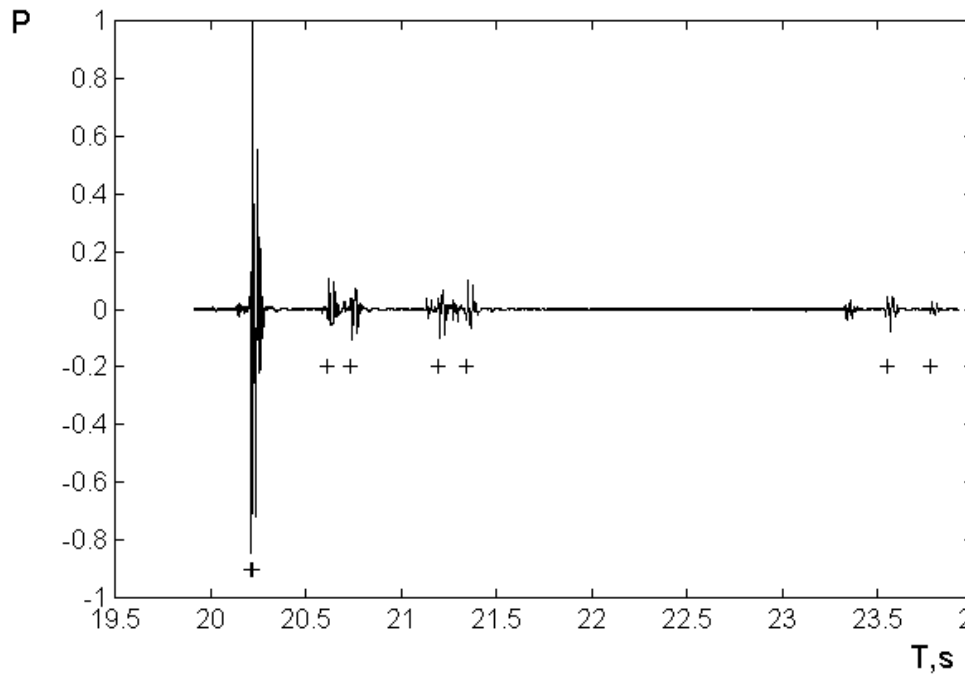


Fig. 2.2 Signal calculated by the PDPE technique.

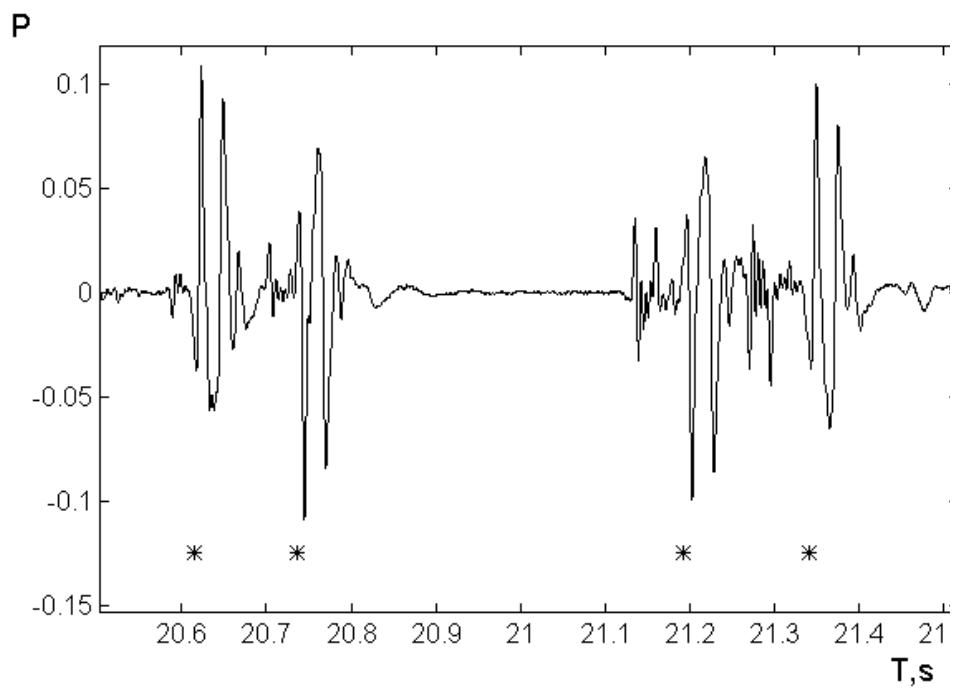


Fig. 2.3. Bottom reflected arrivals - calculation.

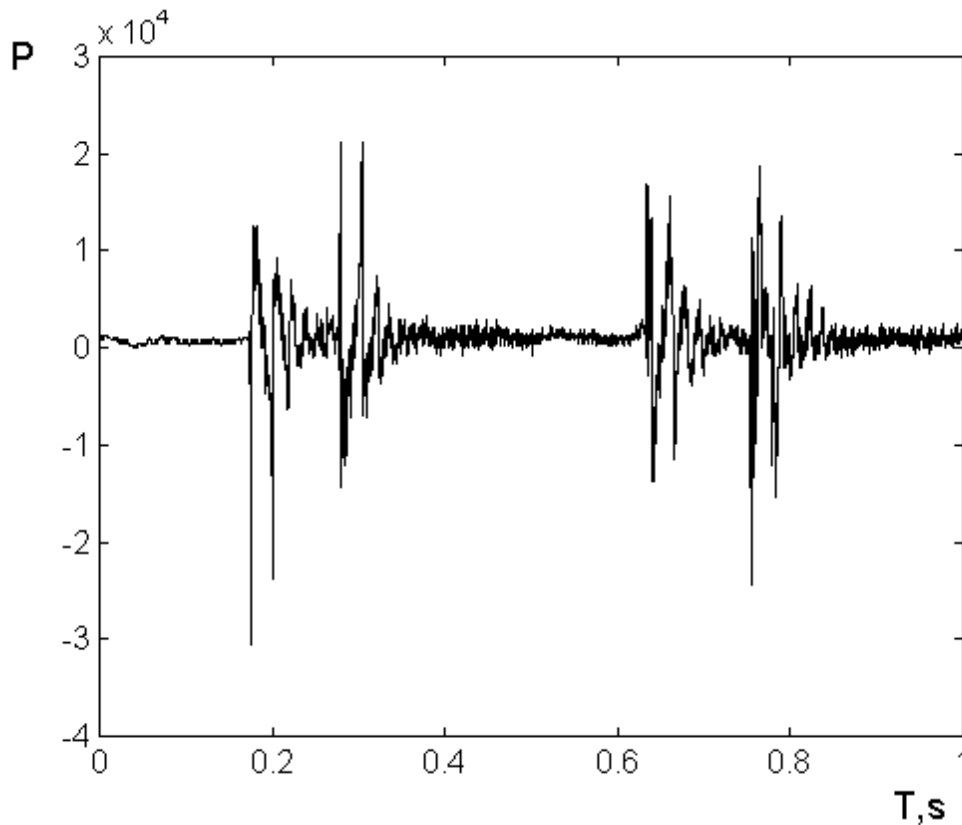


Fig. 2.4 Bottom reflected arrivals - experiment.

Examples of calculation in the range-dependent ocean

Field of the broadband sound source situated on the ocean shelf.

The sound speed and density data both in water and bottom and some experimental and calculated curves in this section are borrowed from the paper *J.H. Beebe, S.?. McDaniel, Geoacoustic models of sea bottom, explaining singularities of sound propagation over the Scotia shelf, in Bottom-Interacting Ocean Acoustics, W.A. Kuperman and F.B. Jensen, Eds., NY and London, Plenum Press.*

Fig. 6, borrowed from this paper shows the profiles of sound speed in water and profile of bottom in considered region of ocean.

Fig. 7 shows the level curves for the sound speed in water, interpolated accordingly the data from Fig. 6, and structure of geological stratum in bottom

Fig. 8 - 11 show the experimental sound levels from underwater explosions for two source depths (represented on figures by ? symbol), sound levels calculated

by the authors of the specified paper by the adiabatic normal mode method (represented on figures by dashed curves) and levels calculated by the PDPE technique (on figures - continuous curves). Experimental points and the calculated curves are obtained in the one-third octave bands with central frequencies 25 and 80 Hz. The receiver is placed at depth 56 m in the beginning of the propagation path. The PDPE results seem to describe the experiment somewhat better than the adiabatic normal mode results.

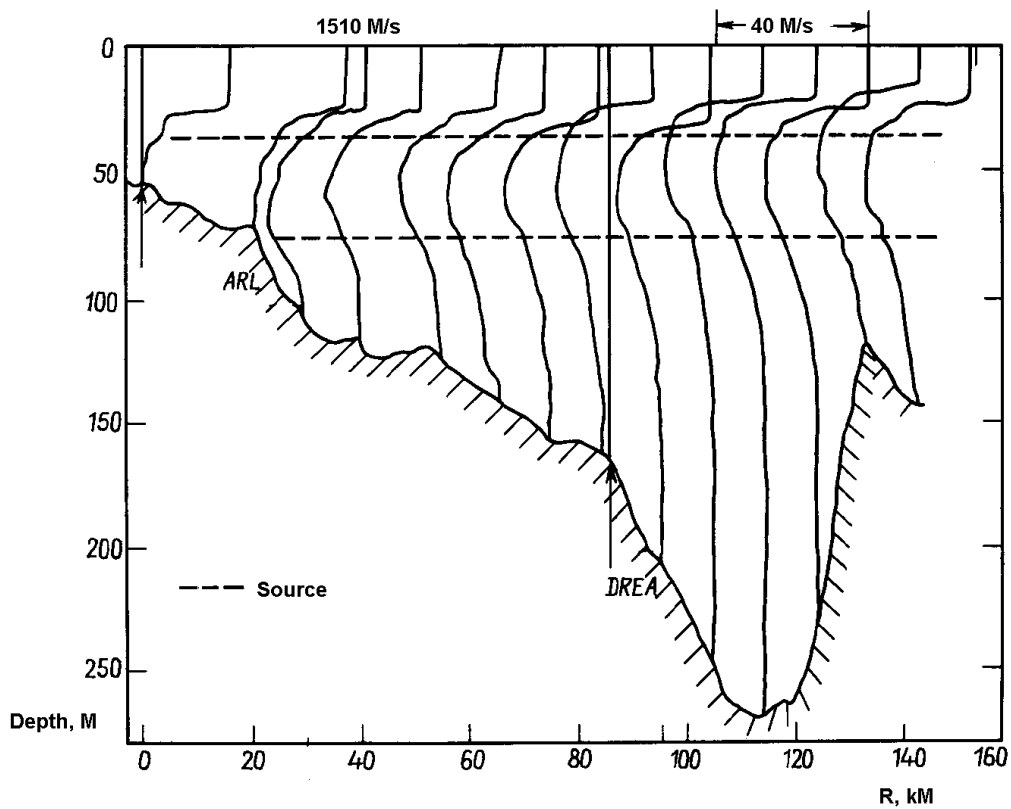


Fig. 6. The sound speed profiles and bottom relief .

Fig. 7. The levels of sound speed in water and structure of bottom layers.

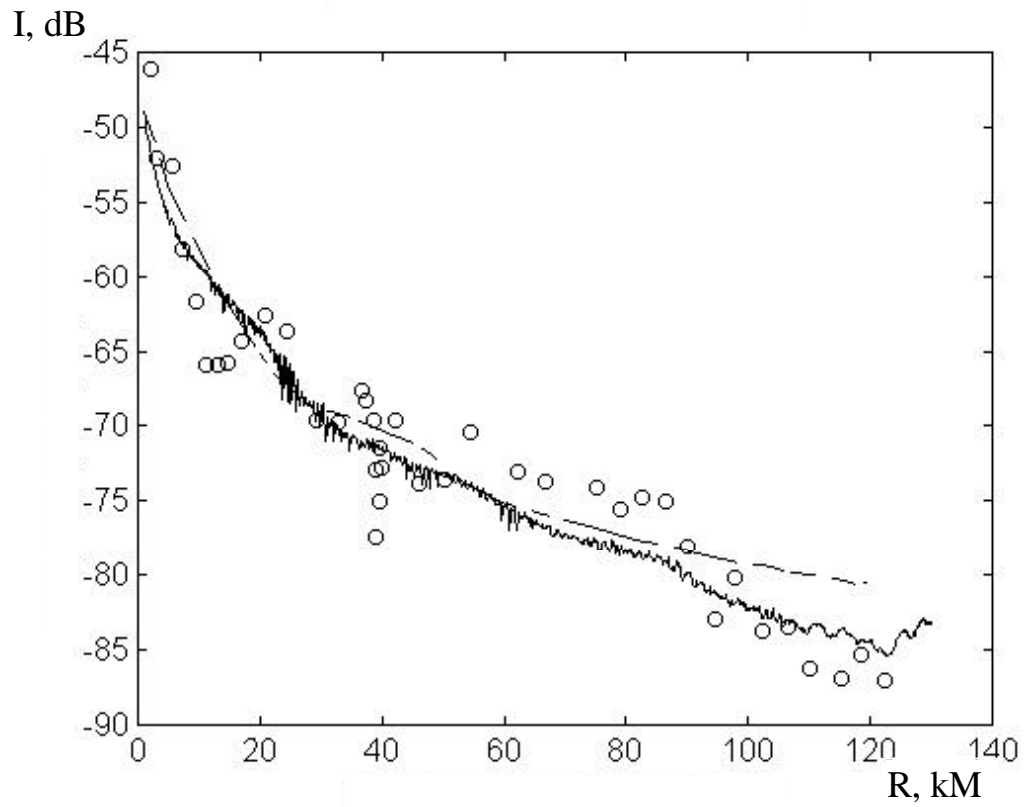


Fig. 8. Transmission losses. The frequency is 25 Hz, the source depth is 38 m.

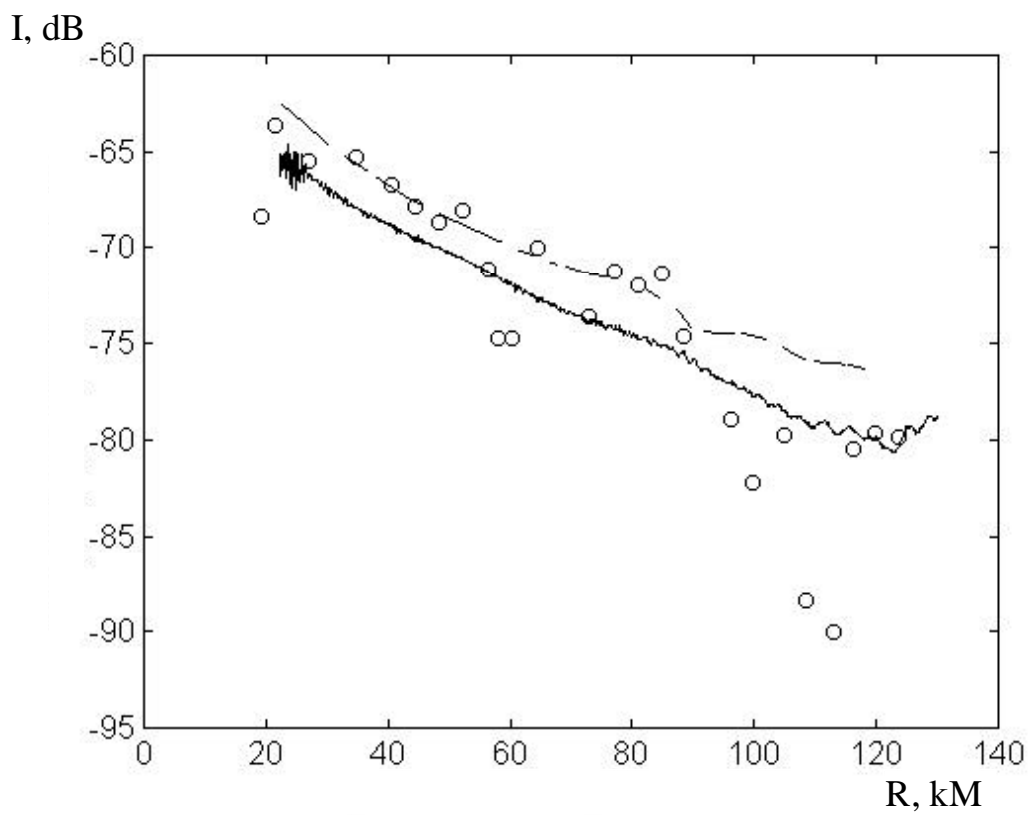


Fig. 9. Transmission losses. The frequency is 25 Hz, the source depth is 79 m.

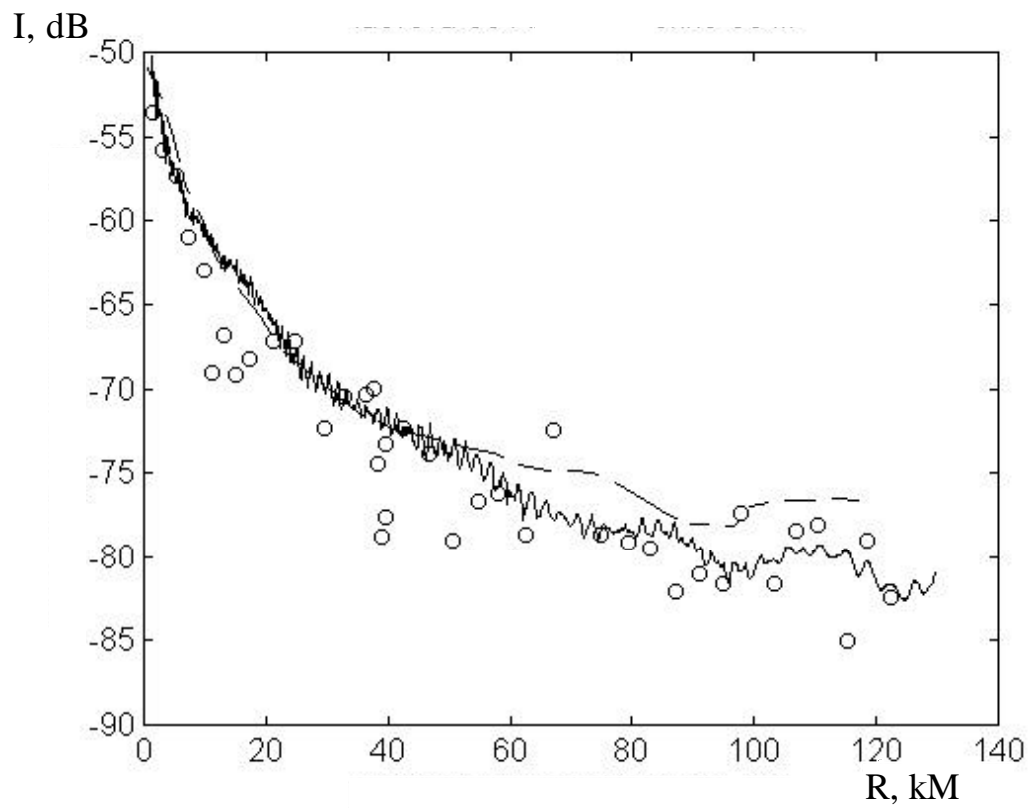


Fig. 10. Transmission losses. The frequency is 80 Hz, the source depth is 38 m.

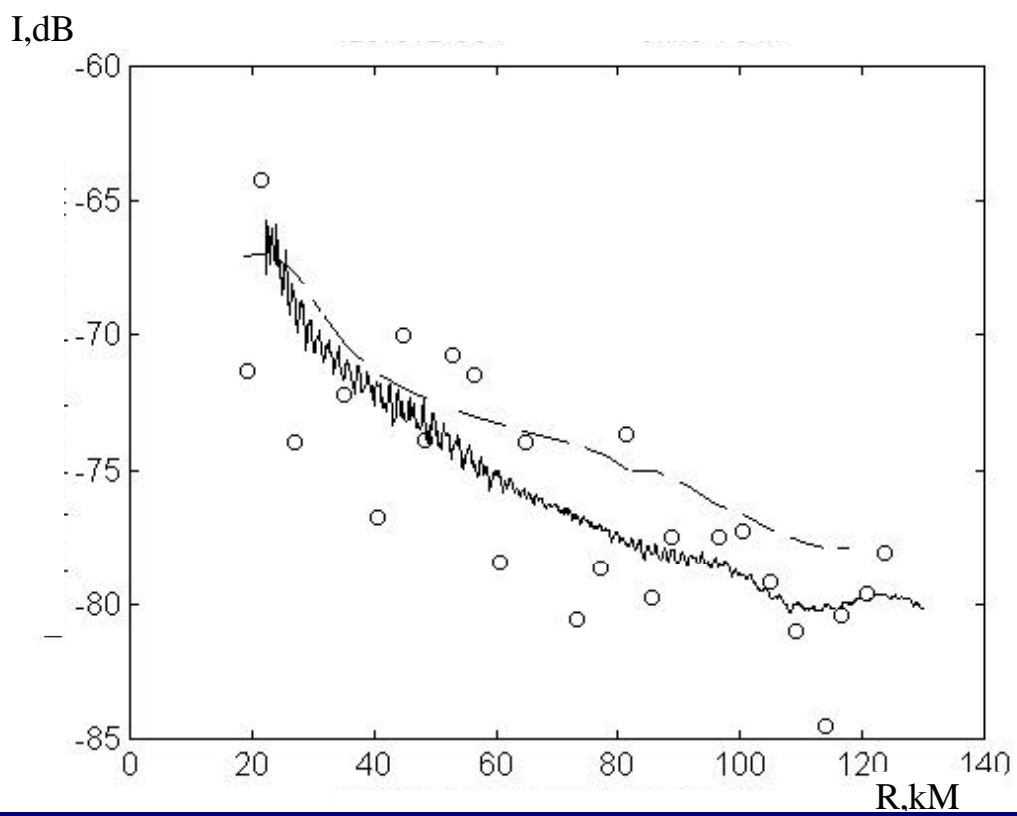


Fig. 11. Transmission losses. The frequency is 80 Hz, the source depth is 79 m.

It should be noted also, that the PDPE technique generates the sound field values in the whole waveguide. Fig. 12 shows the pattern of excess of sound field over the cylindrical losses in the considered model of the ocean shelf in the one-third octave band with central frequency 80 Hz. The highest levels of sound field in water are seen near the axes of the underwater sound channel which depth varies along the propagation path (see. Figs. 6, 7). The sound penetrates the upper acoustically soft bottom layer of sediments and lower by the well expressed intensity structures.

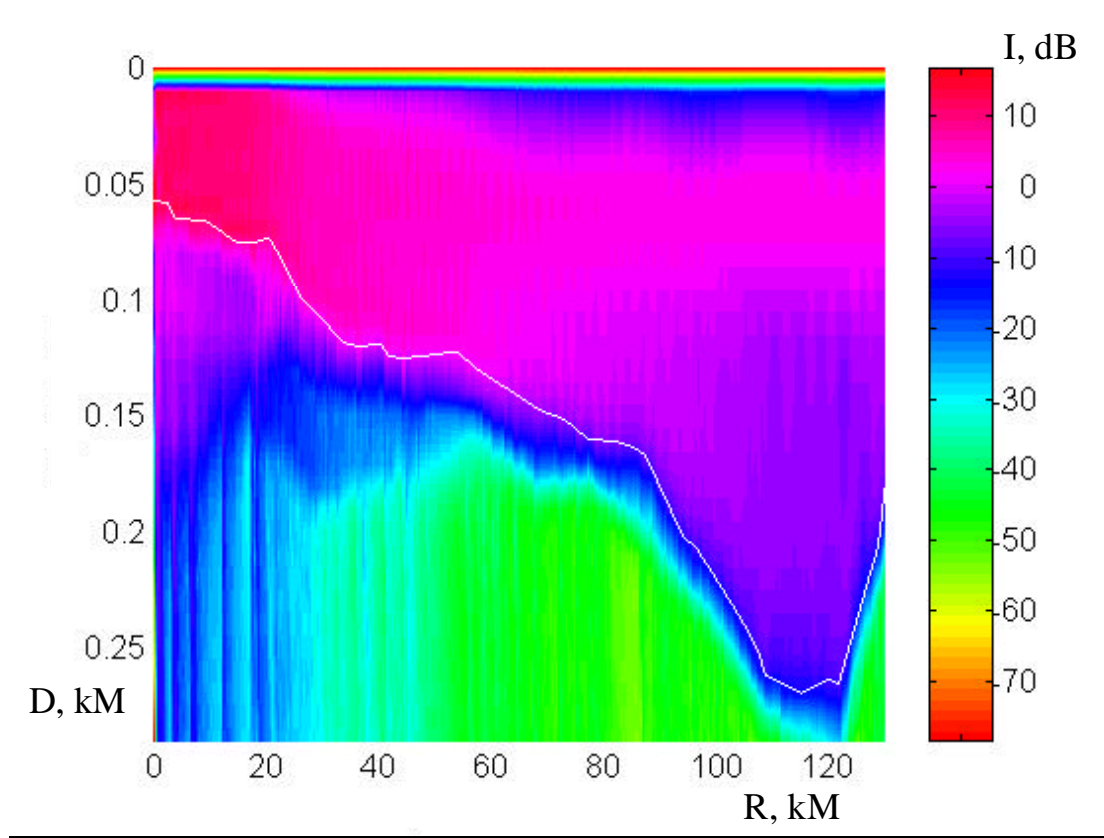


Fig.12. The excess of sound field over the cylindrical losses.

Fig. 13 illustrates the Doppler effect and signal spectrum splitting due to the source motion. The continuous curve represents the spectrum of the signal from the source of harmonic sound with frequency 60 Hz moving with the velocity 10 knots at depth 45m received at depth 6 m for two durations of the analysis: 500 s (solid curve) and 25 s (dashed curve). The source leaves from the receiver, initial distance is 7 km. The curve for the analysis time 500 s exhibits spectrum maxima corresponding to separate normal modes, while the curve for the analysis time 25 s gives only the average Doppler shift of approximately 0.2 Hz.

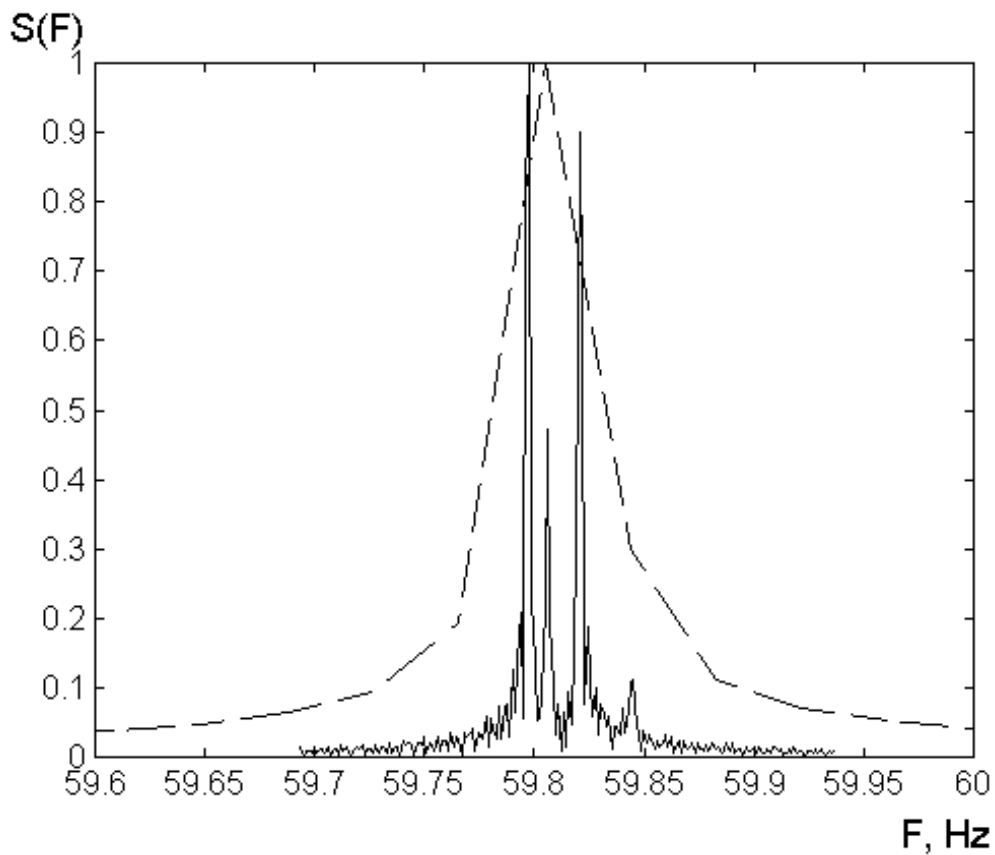


Fig. 13. The spectrum of the signal of a harmonic sound source of frequency 60 Hz moving with the velocity 10 Knots.

Another interesting example concerning acoustic tomography. Fig. 14 shows the levels of sound speed along the transversal slice of Bering Strait in July. Fig. 15 shows the surface of the amplitude of the complex envelope of the impulse response on the vertical receiver array situated at distance 37.05 km from the source lying on the sea floor. The frequency band of the source is 370..420 Hz.

Fig. 16 shows the levels of the same amplitude. One can see the complicated structure of the arrivals of higher normal modes due to their interaction on the range-dependent sea bottom and sound speed.

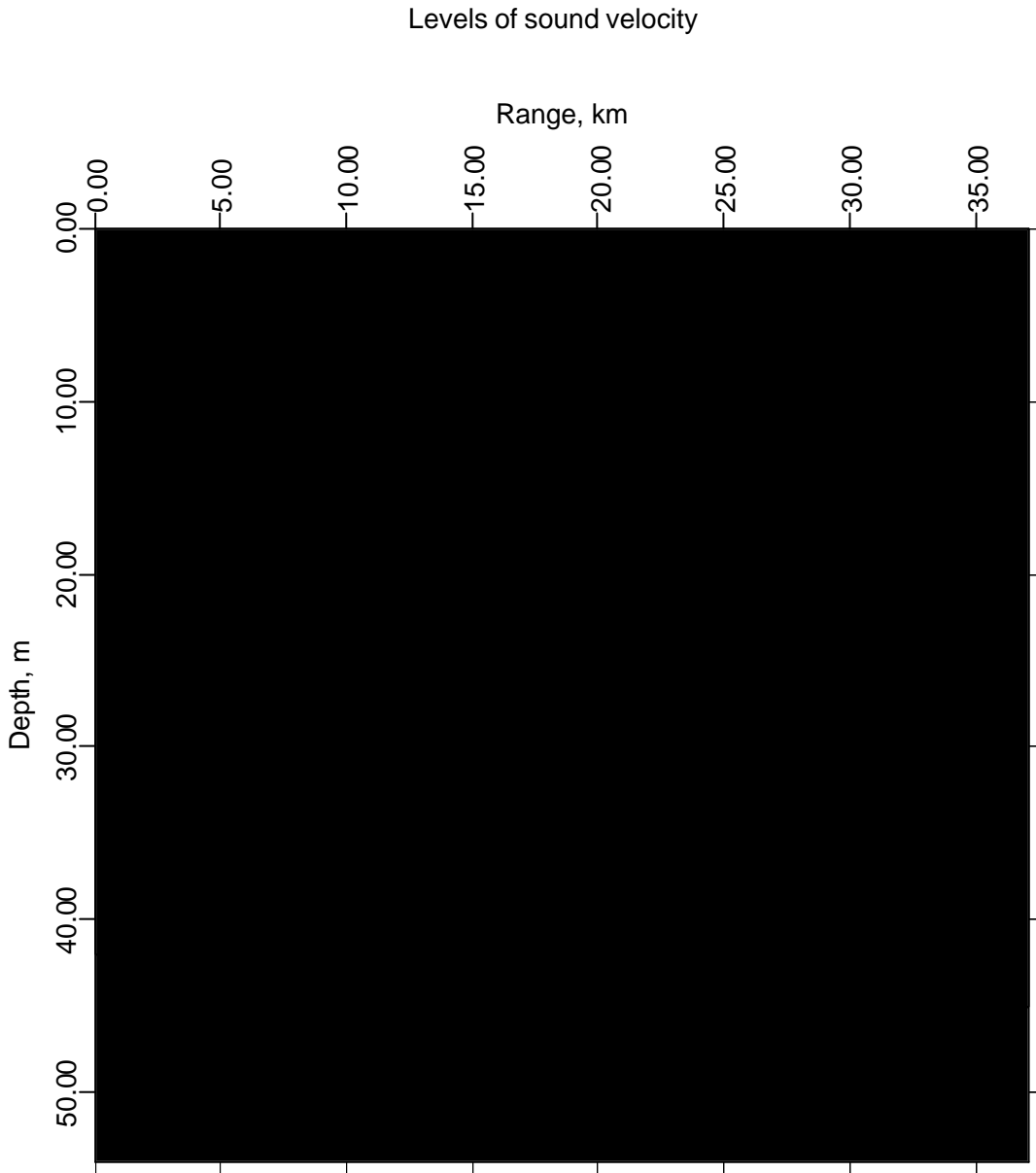


Fig. 14

Amplitude of the complex envelope of the IR against part of the time and depth

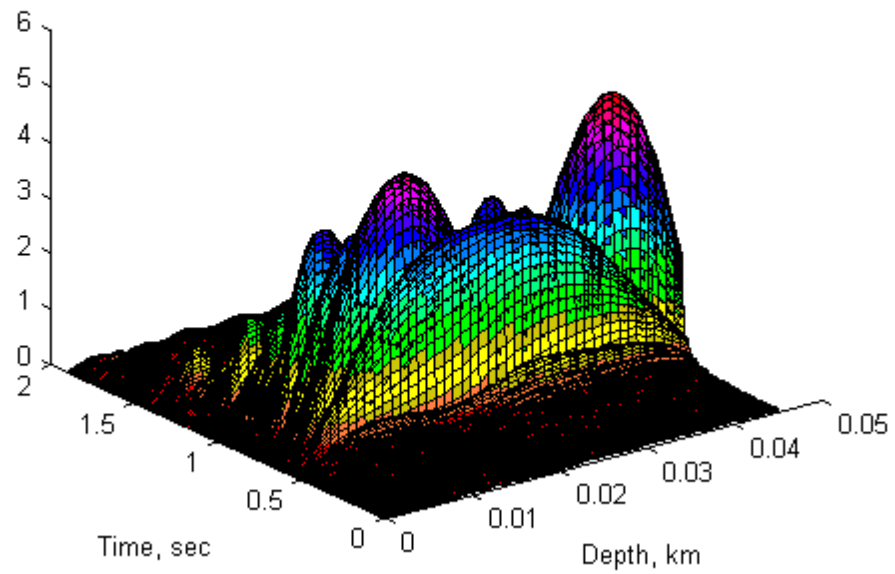


Fig. 15

Amplitude of the complex envelope of the IR against part of the time and depth

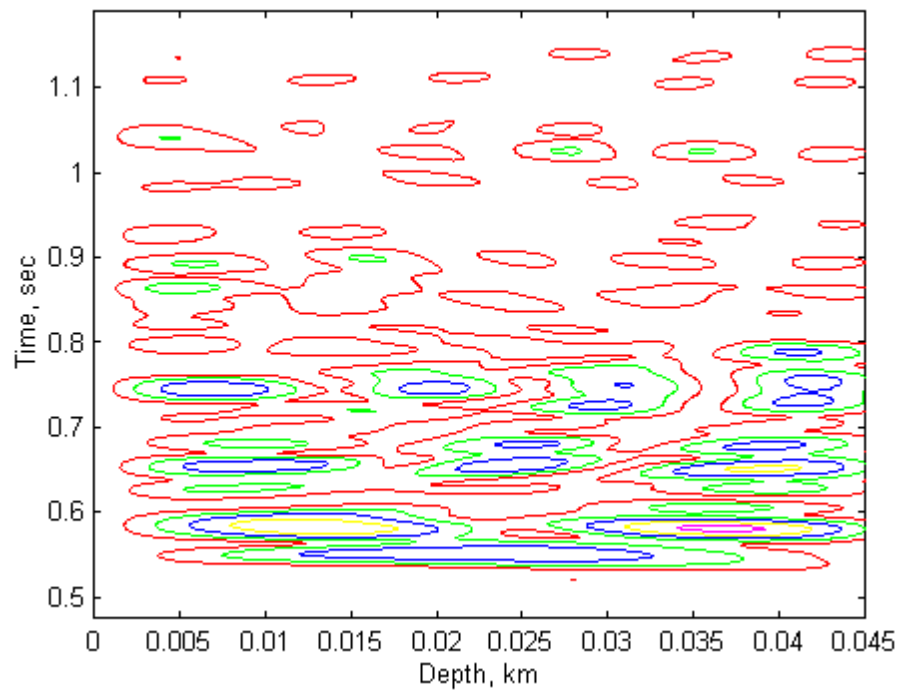


Fig. 16